

3-Phase Rectifier System with very demanding dynamic load

M.R. Ramos, S. Zhao, J.M. Molina, P. Alou, J.A. Oliver, J.A. Cobos

Abstract—This paper presents a distributed power architecture for aerospace application with very restrictive specifications. Additionally, the rectifier switching frequency has to be synchronized with an external frequency clock to minimize the interference of the converter harmonics with the load. In order to protect the 3 phase generator against high load steps, an intermediate bus (based in a high capacitance) to provide energy to the loads during the high load steps is included. Prototypes of the rectifier and EMI filter are built and the energy control is validated.

Index Terms—Power Distribution System, EMI, Energy Control.

I. INTRODUCTION

IN recent years, the topic of the More Electric Aircraft (MEA) has become important [1]-[5]. The More Electric Aircraft (MEA) concept is based on utilizing electric power to drive aircraft subsystems which historically have been driven by a combination of hydraulic, electric, pneumatic, and mechanical power transfer systems. This increases the electric power demand in these aircrafts leading to a need for compact and efficient power converters for aircraft applications and a resulting research focus in this area [6]. Normally the power conversion system consists of two main stages: a Three-phase AC/DC rectifier (including EMI filter) which mainly takes charge of achieving good power factor (PF) and low THD at the input; and a second stage consisting of an isolated DC/DC converter to supply the load equipment, which aims at ensuring fast dynamic response and meanwhile meeting the desirable output specifications [7][8].

The system analyzed in this paper has an intermediate bus, based on a high capacitance. The intermediate bus is included to protect the generator during high load steps. An energy control method is proposed that utilizes the energy stored in the output capacitor rectifier to control the output voltage of the rectifier. In such a way, the minimum bandwidth restriction imposed by the RHP pole of the power load is eliminated and the bandwidth of the voltage loop can be defined slow enough to demand smooth power from the generator.

In section II the architecture of an AC/DC system formed by seven independent loads supplies from an 115V 400Hz generator with a total power of 13kW is presented.

In section III a Control Strategy to protect the generator against high load steps is proposed.

In section IV the validation of the control and the experimental results are shown.

II. POWER SYSTEM ARCHITECTURE

A. System Specifications

The system has to comply with the followings specifications:

- Input Voltage: 115V RMS phase to neutral point
- Main frequency: 400Hz
- Nominal Bus Voltage(V_o): 200 V
- Range of Bus Voltage (V_o): 180V to 250 V
- Rated output power: 13 kW
- Comply with MIL-STD-704F
- Comply with MIL-STD-461E
- Military derating
- Galvanic isolation
- Ambient temperature: 70 °C
- Switching Frequency externally synchronized

The Military derating that has been considered is: 70 % in diodes voltage, 75 % in transistor current, 70 % in transistor voltages and 110 °C as maximum temperature in magnetic cores.

To achieve galvanic isolation the system is divided in two stages, a rectifier stage and a DC/DC stage with isolation.

B. Power Architecture

The system is equipped of an intermediate bus between the rectifier and the DC/DC. This bus provides the energy demanded by the load during high load steps. The basic structure of the system is shown in Fig. 1.

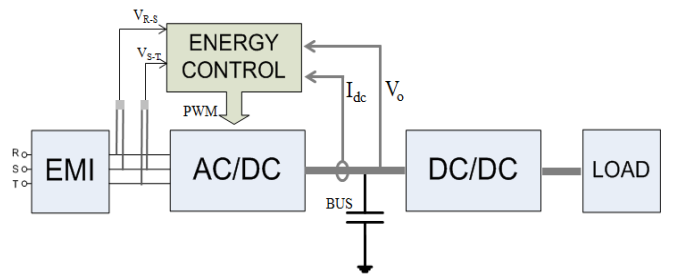


Fig. 1. Block diagram of the system

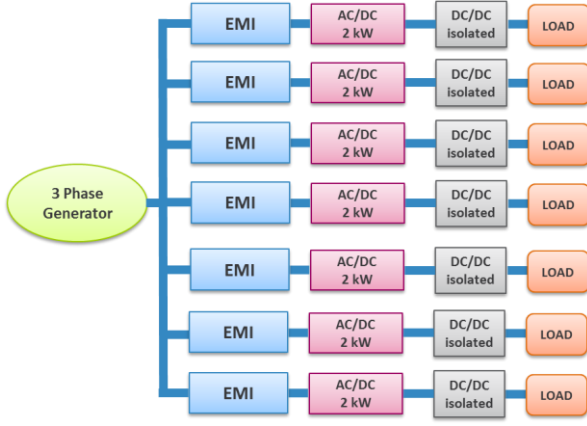


Fig. 2. Designed architecture of the 13kW rectifier system

This architecture has 7 distributed channels (Fig. 2). The modularity of this solution enhances the reliability. Each channel is formed by the EMI filter, two power stage and one intermediate bus (Fig. 1).

To obtain a high power density and high efficiency, the three phase buck-type rectifier has been selected because it can provide a wide output voltage range down to low voltages maintaining good power factor at the input.

The control of the rectifier is analyzed in detail in Section III. For this application a Full-Bridge Phase Shift (FBPS) has been selected. FBPS is a very popular topology in the range of a few kilowatts [9]. The specifications of galvanic isolation and high power density are satisfied with this topology.

The system analyzed in this paper is based in seven FBPS of 2 kW.

The EMI filter has three stages of differential mode and one common mode stage for each channel.

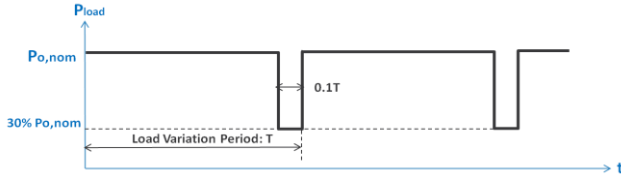


Fig. 3. Characteristic of the Load Steps

III. CONTROL STRATEGY

A. Motivation

Conventional three-phase rectifiers are controlled to achieve good power factor and low THD in the input. In this conventional control method discussed in [10], an inner DC inductor current loop and an outer output voltage loop [11] are implemented based on a resistive load; where as in this application the rectifier is loaded with a DC/DC converter operating as a constant power source at steady state, with impose more restrictions in the control design. Notably in this application, the DC/DC Full-Bridge with its load device present a periodically dynamic power profile (Fig.3). Therefore for the sake of enlarging the life span of the aircraft generator under these high power steps, an energy control

method is proposed to control the rectifier with low bandwidth in order to demand smooth power from the generator while abrupt load steps happen. Meanwhile, by the proposed method, the constraint of the right half plane pole brought by the constant power load is eliminated. Therefore the control bandwidth can be configured low enough to protect the generator. This slow energy control (Fig. 4) method penalizes the output capacitance, because the power unbalance during the transient can only be handled by the output capacitance.

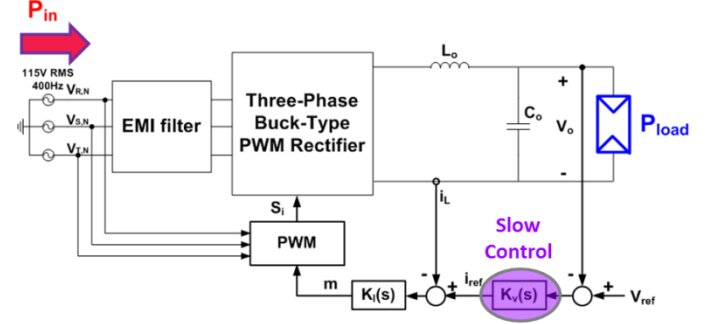


Fig. 4. Schematic of the proposed slow-bandwidth control loop

B. Conventional Control of Three-Phase Buck Type Rectifier

As stated above, the aim of the proposed method is to control the rectifier to demand smooth power from the generator under a pulsating power load. It implies that the control loop should be slow enough, that the abrupt load step does not provoke the rectifier to react immediately.

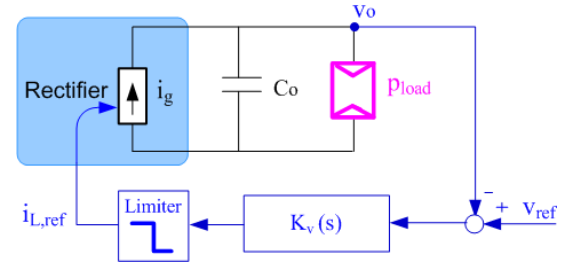


Fig. 5. Simplified model of a current controlled buck rectifier with conventional outer voltage loop.

Starting from the conventional modeling approach for the three-phase buck-type rectifier [10], it is generally modeled as current source with values I_g which denotes the average inductor current in the output filter and assuming that it can be controlled fast enough to track the current reference $i_{L,ref}$ through an inner inductor current loop (not shown in Fig. 5). Moreover, an outer slower voltage control loop (shown in Fig. 5) is usually implemented. Meanwhile the DC/DC with its load is represented as power source P_{load} . Thus in this case at steady state, the plant model of the rectifier in Fig.5 can be described as

$$C_o \frac{dv_o(t)}{dt} = i_g(t) - \frac{P_{load}(t)}{v_o(t)} \quad (1)$$

At a certain operating point, the small-signal open-loop transfer function of v_o/i_g can be derived as

$$\frac{\hat{v}_o(s)}{\hat{i}_g(s)} = \frac{-R_{eq}}{1 - R_{eq}C_o \cdot s} \quad (2)$$

where R_{eq} denotes the load equivalent resistance at operating point,

$$R_{eq} = \frac{V_{o,nom}^2}{P_{o,nom}^2} = \frac{200V^2}{13000W} = 3.077\Omega \quad (3)$$

Obviously, the negative equivalent load resistance in the denominator of (2) implies a right half plane pole in the open loop transfer function which is open-loop unstable. In order to ensure stability, according to Nyquist Stability Criterion [12], it is necessary to implement a controller with a loop gain big enough to make the contour encircle point $(-1, j0)$ counterclockwise in the Nyquist plot [13]. Accordingly this feature prevents the control loop from going even slower since the loop bandwidth is constrained by $BW > \frac{2}{2\pi R_{min}C_o}$ (R_{min} implies values of the minimum equivalent load resistance at maximum power)

C. Proposed Energy Control Method

As mentioned above, the preferred control strategy should have a slow bandwidth.

Thus, another transfer function is derived with a term $v_o(t)$ multiplied to both sides of (1);

$$v_o(t)C_o \frac{dv_o(t)}{dt} = v_o(t)i_g(t) - p_{load}(t) \quad (4)$$

Notably, $v_o(t)C_o \frac{dv_o(t)}{dt}$ happens to be the derivative of energy in the output capacitance over time. Thus, there stands

$$\frac{d\varepsilon_c(t)}{dt} = p_g(t) - p_{load}(t) \quad (5)$$

It is straight forward to obtain the transfer function of $\varepsilon_c(s)$ over $p_g(s)$ like

$$\frac{\hat{\varepsilon}_c(s)}{\hat{p}_g(s)} = \frac{1}{s} \quad (6)$$

If the rectifier is controlled as a power source during the load transients and, instead of controlling the bus voltage (V_o), the energy stored in C_o is controlled, based on the plant model of Eq. (6), thus, there is no restriction in the decision of the system bandwidth, being a trade-off between the energy stored in C_o and the load transient demanded to the three phase generator. As a result, in the following control alternatives, the energy in the output capacitance is monitored and used to control the power injected through the rectifier. This idea comes from passivity based control [13]. Here, two different type of controllers based on the issue of slow energy control loop are discussed.

1) Outer Energy Control Loop

Based on the plant model in (6), a PI controller for the outer capacitor energy loop can be implemented as shown in the block diagram in Fig. 6. By adjusting the gains of the PI

controller, different control bandwidths can be reached without restriction on stability issues.

As can be seen, the output capacitance C_o is a crucial component in the rectifier system. Especially under the condition of a low-bandwidth control, while a load step happens, the power unbalance between the load and the smoothly varied input power demanded from the generator can only be handled by the output capacitor C_o . This naturally results in a variation on V_o . While deciding the bandwidth value, the minimum value for C_o has to be concerned, since volume and weight, as well as cost are important in all applications especially in aircraft applications.

Obviously, there is a trade-off between ΔP_{in} , C_o and ΔV_o . This is because slower control loop (i.e. smaller ΔP_{in}) brings bigger P_{in} - P_{out} unbalance during transients, which requires bigger C_o value to handle, meanwhile keeping V_o inside the nominal range. Thus a PI controller for outer energy loop with a bandwidth of 0.16Hz is designed to meet the desired ΔP_{in} value. The transient response of the averaged model simulation is shown in Fig. 7, where an input phase RMS current variation $\Delta I_{in,rms}=4.5A$ (only 12% of nominal input phase RMS current is obtained.)

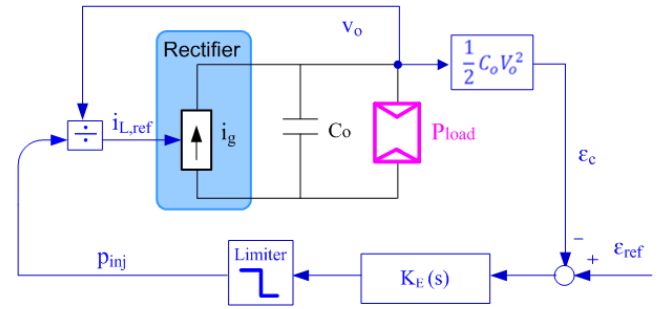


Fig. 6. Simplified model of the proposed outer energy control loop.

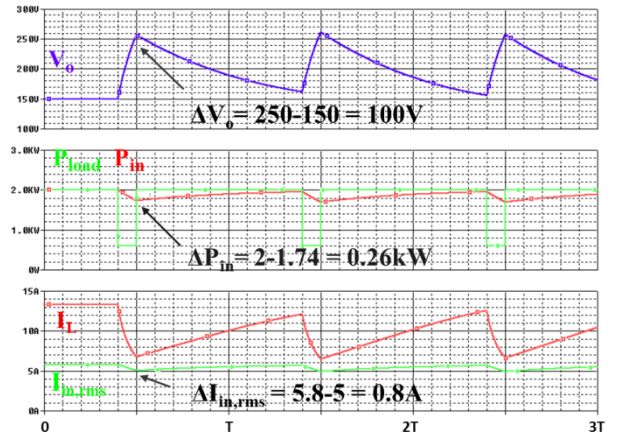


Fig. 7. Transient response of the proposed control at bandwidth of 0.16Hz.

2) Inner DC Current Loop

With the method stated above, according to (5) the outer energy control loop is able to adjust P_{inj} equivalent to P_{load} at steady state by controlling ε_c . Thus, for the inner inductor current loop design, the load can be considered as an equivalent positive resistive load. Then, the plant transfer

fuction for the inductor current (i_L) versus modulation index (m) [14].

$$G_{i_L/\tilde{m}}(s) = \frac{U_{N,eq}}{R_{nom}} \cdot \frac{R_{nom}C_o \cdot s + 1}{L_o C_o \cdot s^2 + \frac{L_o}{R_{nom}} \cdot s + 1} \quad (7)$$

where $U_{N,eq}$ refers to the equivalent DC input voltage [11] with $U_{N,eq} = \frac{3}{2} \hat{U}_N = 244V$, and $L_o = L_{o+} + L_{o-} = 150\mu H$. According to this plant model, a PI controller is adopted in the inner inductor current control loop with a bandwidth of 4.2kHz.

Then by the switching model simulation, a step reference response for the average inductor current from 7A to 10A is captured in Fig. 8, consequently V_o varies from 140V to the new steady state of 200V. The graph shows that the inner DC current controller is able to track the reference for the average inductor current immediately.

3) Over-voltage Protection Scheme

In reality, for this unidirectional buck-type rectifier, the maximum controlled output voltage is 244V. When V_o is higher than 244V (according to $V_o = M \cdot \frac{3}{2} \hat{U}_N$ where $M=1$), the rectifier cannot control the power delivered to the load. Thus, an over-voltage protection scheme is designed to ensure that V_o does not exceed an upper limit (set at 215V in this case). The protection scheme is achieved as following: first is to set the maximum output voltage reference $V_{ref,max} = 215V$ which is related to the maximum capacitor energy reference $E_{ref,max} = \frac{1}{2} C_o \cdot V_{ref,max}^2$. Second, when V_o goes over $V_{ref,max}$, the control bandwidth is increased to have a faster energy loop that regulates V_o at the upper limit; while V_o stays inside the nominal range, the designed 0.16Hz small-bandwidth loop takes effect.

Fig. 9 shows the switching model simulation of the 2kW rectifier cell with the proposed over-voltage protection scheme implemented. It can be seen that, when load step happens, the outer energy control loop is working with a small-bandwidth which controls P_{in} to respond smoothly. Once V_o exceeds 215V, the high-bandwidth energy loop is activated which makes p_{in} react fast to P_{load} and thereby clamps V_o inside the regulation band. Accordingly, $i_{in,phase}$ is varying smoothly while a load step occurs and after entering the protection

mode, the loop reacts fast to demand the balance between P_{in} and P_{load} .

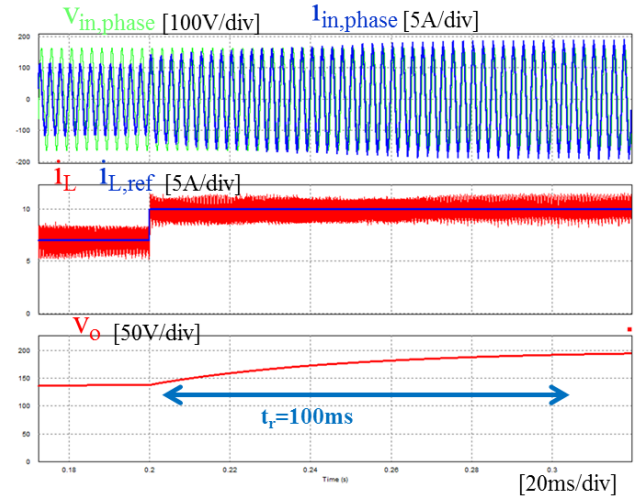


Fig. 8. Simulation of reference step response of the inner DC current loop from 7A to 10A with the designed PI controller

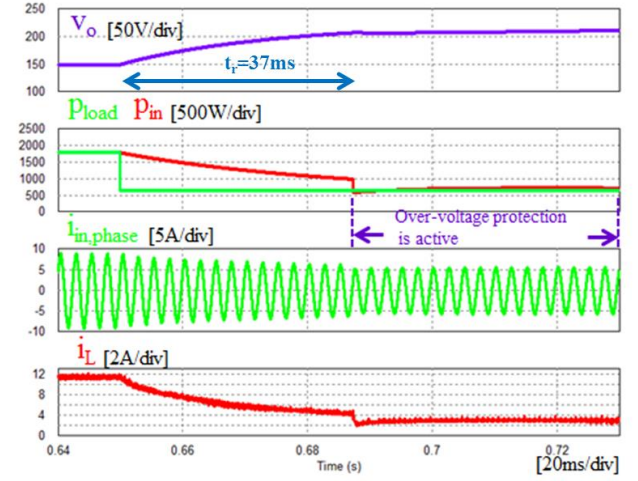


Fig. 9. Transient response for switching model simulation applying over-voltage protection.

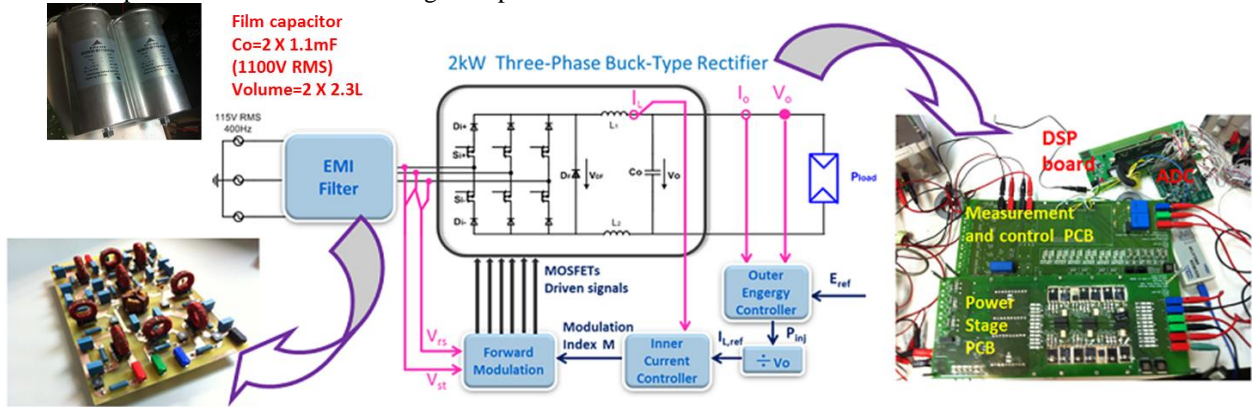


Fig. 10. Complete control schematic with prototype pictures.

IV. EXPERIMENTAL RESULTS

A 2kW 3 phase buck type rectifier and an EMI filter has been built in order to validate the energy control and verify that the architecture comply with the system specifications. Also the proposed energy control method has been implemented as shown in Fig. 10. Digital control is employed with a TI TMS320C28346 DSP experimenter's kit [15] and a TI ADS8556 ADC evaluation module [16].

As stated above, the slow bandwidth control loop penalizes the output capacitance. That is to say, for a fixed v_o variation range, the bigger the capacitance, the slower the bandwidth can be reached. In order to minimize volume and weight in aircraft applications, considering the state-of-the-art, electrolytic capacitors always show the best energy density and applicable quantities over other technologies (e.g. ceramic, film, etc.). Also for the sake of availability, in the 2kW rectifier prototype, two film capacitors from EPCOS B25620B1118K103 [17] are installed at the output of the rectifier prototype. Each of the capacitor is 1.1mF, with volume of 2.4L and rated voltage of 1100V. All the experimental results are done with $C_o=2.2\text{mF}$.

Fig. 11 presents the open loop measurement of the rectifier operating at maximum output power of 2kW with $V_o=200\text{V}$ (fixed modulation index of 0.82) supplying resistive load of 20 Ω . The THD is 6% and PF is 0.98 (measured with Yokogawa WT1800 Power Analyzer [18]), and the overall efficiency including the EMI filter is 95%.

As to the inner DC current loop, Fig. 12 presents a 7A to 10A reference step response on the resistive load of 20 Ω . It can be seen that the experimental results match the switching model simulation, i.e., inductor current is able to track the step reference quickly.

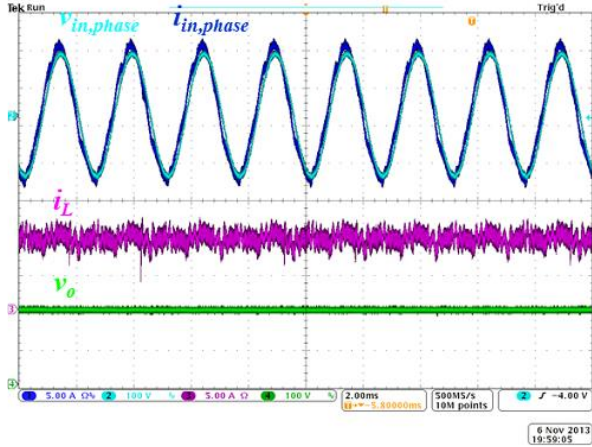


Fig. 11. Open loop measurement of the rectifier system at 2kW, with resistive load(20 Ω), $V_{in,phase}$ [100V/div], $i_{in,phase}$ [5A/div], i_L [5A/div], v_o [100V/div].

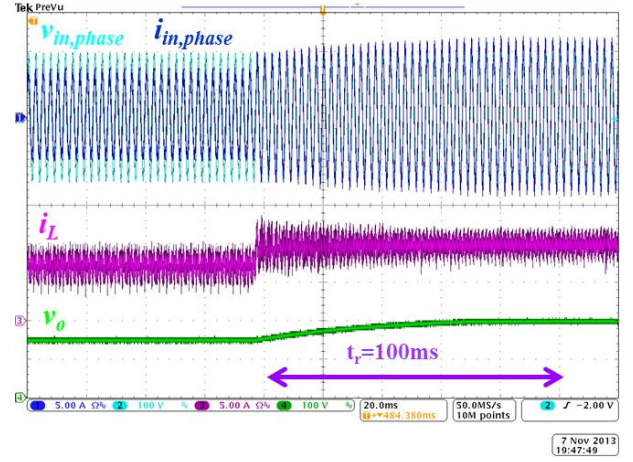


Fig. 12. Measurement of inner DC current loop reference step tracking from 7A to 10A, with resistive load(20 Ω), $V_{in,phase}$ [100V/div], $i_{in,phase}$ [5A/div], i_L [5A/div], v_o [100V/div].

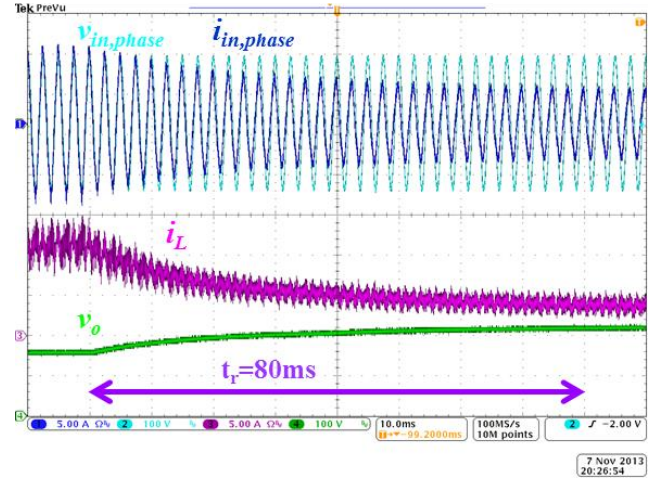


Fig. 13. Measurement of energy loop working under power load step from 1.8kW down to 650W, i_{in} is controlled to vary smoothly and consequently causes v_o to increase slowly from 150V to 220V. $V_{in,phase}$ [100V/div], $i_{in,phase}$ [5A/div], i_L [5A/div], v_o [100V/div].

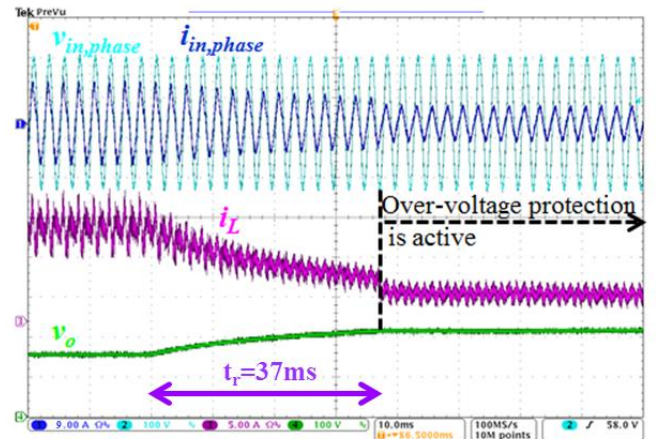


Fig. 14. Over-voltage protection scheme is triggered when v_o is beyond 215V during the load step, meanwhile energy loop bandwidth is changed into a bigger value in order to control p_{in} quickly converged to p_{load} , $V_{in,phase}$ [100V/div], $i_{in,phase}$ [9A/div], i_L [5A/div], v_o [100V/div].

Experimental results in Fig. 13 verify the energy loop working under an electronic load (Chroma DC Electronic Load 63204 [19]) of constant power mode for a fast load step from 1.8kW to 650W. It can be seen that after the load step happens, the RMS value of $i_{in,phase}$ is decreasing slowly which also suggests the input power is reducing smoothly and finally after a time interval of 80ms, V_o varies from 150V to the new steady state of 220V. Thereafter, P_{in} is equivalent with P_{load} which maintains the balance on the E_c (related to V_o). Besides, the average value of i_L is decreasing, which is controlled by the desired $i_{L,ref}$.

According to the over-voltage protection scheme designed in section III.3, an experimental result is shown in Fig. 14. The limit to trigger the protection scheme is configured to 215V in this experiment. It is obvious that once V_o varies over the 215V boundary, the bandwidth of the energy control loop is changed to a higher value and therefore V_o is kept constant while P_{in} quickly converges to P_{load} . Consequently a new steady state of $i_{in,phase}$ and i_L is maintained thereafter.

V. CONCLUSION

The power architecture and the energy control strategy for a 13kW system have been analyzed and presented in this paper.

Three critical specifications make this system very different from typical applications:

- 1) The switching frequency must be synchronized with an external reference which can range between 80 kHz-130 kHz and multiples.
- 2) The loads have a demanding transient behavior, changing from 4 kW to 13 kW.
- 3) To increase the reliability of the three phase generator, it is proposed to protect the generator from the load steps by increasing the output capacitance of the rectifier and slow down the bandwidth of the control.

The output voltage of the rectifier cannot be controlled with a classical control since it is loaded with a power source, creating a right half plane pole in the system and making mandatory a high bandwidth to stabilize the system. The paper proposes to control the rectifier as a power source and controlling the energy of the output capacitance instead of the output voltage. Applying this control, the RHP pole is eliminated, becoming the bandwidth a free design variable and making possible the use of a slow bandwidth in the system. As a result, with the same $C_o=5.8mF$, an energy control loop of 0.16Hz bandwidth (30 times smaller than 4.8Hz) with $\Delta I_{in,rms}=0.8A$ (only 13.8% of nominal input phase RMS current) is designed and verified at simulation level.

A prototype of a 2kW rectifier cell is built together with the inner loop for modulation of the six switches. Experimental results for $P_o=2$ kW are shown.

REFERENCES

- [1] R.D. Telford, S. Galloway, and G. M. Burt "Evaluating the reliability amp; availability of more-electric aircraft power system," in *Universities Power Engineering Conference (UPEC)*, 2012 47th International, 2012, pp. 1-6.
- [2] R. I. Jones, "The more electric aircraft: the past and the future?" in *Electrical Machines and Systems for the More Electric Aircraft (Ref. No. 1999/180)*, IEE Colloquium on 1999, pp.1/1-1/4.
- [3] J. S. Cloyd, "Status of the united states air force's more electric aircraft initiative," *IEEE Aerospace and Electronic Systems Magazine*, vol. 13, no. 4, pp. 17-22, 1998.
- [4] W. G. Homeyer, E. E. Bowles, S. P. Lupan, P. S. Walia, and M. A. Maldonado, "Advanced power converters for more electric aircraft applications," in *Proc. 32nd Intersociety Energy Conversion Engineering*
- [5] D. Izquierdo, R. Azcona, F. del Cerro, C. Fernandez, and B. Delicado, "Electrical power distribution system (hv270dc), for application in more electric aircraft," in *Proc. Twenty-Fifth Annual IEEE Applied Power Electronics Conf. and Exposition (APEC)*, 2010, pp. 1300-1305.
- [6] M. Hartmann, "Ultra-compact and ultra-efficient three-phase pwm rectifier systems for more electric aircraft," Ph.D. dissertation, ETH Zurich, 2011.
- [7] M.Silva, N. Hensgens, J.M. Molina, M. Vasic, J. Oliver, P. Alou, O. Garcia, J.A. Cobos, "Interleaved multi-cell isolated three-phase PWM rectifier system for aircraft applications," *Applied Power Electronics Conference and Exposition (APEC)*, 2014 Twenty-Ninth Annual IEEE, vol., no., pp. 1035,1041, 17-21 Mar. 2013.
- [8] T.B. Soeiro, F.Vancu, J.W. Kolar, "Hybrid Active Third-Harmonic Current Injection Mains Interface Concept for DC Distribution Systems," *Power Electronics, IEEE Transactions on*, vol.28, no.1, pp.7-13, Jan. 2013.
- [9] J.A. Sabate, V. Vlatkovic, R.B. Ridley, F.C. Lee, B.H. Cho, "Design considerations for high-voltage high-power full-bridge zero-voltage-switched PWM converter," *Applied Power Electronics Conference and Exposition*, 1990. APEC '90, Conference Proceedings 1990., Fifth Annual , vol., no., pp.275-284, 11-16 March 1990.
- [10] T. Nussbaumer, G. Gong, M.L. Heldwein, J.W. Kolar, "Control-oriented modeling and robust control of a three-phase buck+boost PWM rectifier (VRX-4)," *Industry Application Conference*, 2005, Fourtieth IAS Annual Meeting. Conference Record of the 2005, vol. 1, pp. 169-176, Oct. 2005.
- [11] T. Nussbaumer, and J.W. Kolar "Comparative evaluation of control techniques for a three-phase three-switch buck-type AC-to-DC PWM converter system," *Nordic Workshop on Power and Industrial Electronics (NORPIE '02)*, Aug. 2002.
- [12] R. C. Dorf, R. H. Bishop, *Modern Control Systems*, 12th edition, Pearson, 2010.
- [13] J. S. Freudenberg, D. Looze, "Right half plane poles and zeros and design tradeoffs in feedback systems," *Automatic Control, IEEE Transactions on*, vol.30, no. 6, pp. 555,565, Jun. 1985
- [14] J. Doval-Gandoy, and C. M. Penalver. "Dynamic and steady state analysis of a three phase buck rectifier." *Power Electronics, IEEE Transaction on*, vol. 15, no. 2, pp. 953-959, Nov. 2000.
- [15] Texas Instruments, TMS320C28346 Micro Controller, Tech. Rep., 2012. [Online]. Available: <http://www.ti.com/product/tms320c28346>
- [16] Texas Instruments, ADS8556 ADC Evaluation Module, Tech. Rep., 2009. [Online]. Available: <http://www.ti.com/tool/ADS8556EVM>
- [17] EPCOS, B25620B1118K103 Film Capacitors, Tech. Rep., 2014. [Online]. Available: <http://www.epcos.com/inf/20/50/ds/B2562.pdf>
- [18] YOKOGAWA, WT1800 High Performance Power Analyzer, Tech. Rep., [Online]. Available: <http://tmi.yokogawa.com>
- [19] Chroma, DC Electronic Load 63204, Tech. Rep., 2014. [Online]. Available: <http://www.chromausa.com/pdf/Br-63200-dcload-082014.pdf>